Available online at www.sciencedirect.com
ScienceDirect
Thermochimica Acta 470 (2008) 98–104
thermochimica acta
www.elsevier.com/locate/tca

Nonisothermal crystallization kinetics of amorphous $Te_{51.3}As_{45.7}Cu_3$

A.A. Joraid *, A.A. Abu-Sehly [1], M. Abu El-Oyoun [1], S.N. Alamri

Department of Physics, Taibah University, Madinah, Saudi Arabia

Received 30 November 2007; received in revised form 4 February 2008; accepted 7 February 2008
Available online 10 March 2008

Abstract

The structure and kinetics of the crystallization reaction of amorphous $Te_{51.3}As_{45.7}Cu_3$ were studied under nonisothermal conditions using scanning electron microscopy (SEM) and differential scanning calorimetry (DSC). Two exothermic changes were reported. Five isoconversional methods, of Kissinger–Akahira–Sunose (KAS), Flynn–Wall–Ozawa (FWO), Tang, Starink, and Vyazovkin, were used to determine the variation of the activation energy for crystallization with temperature, $E_\alpha(T)$. The results show that the activation energy for crystallization associated with the first peak first decreases with increasing temperature and then increases. Different behaviour was observed for the second peak, where an increase of E_α with temperature followed by a decrease. The effect of heating rate on the reaction model, $g(\alpha)$, was also different for the two crystallization peaks.

Keywords: Crystallization kinetics; DSC; SEM; Thermal analysis; Annealing effect; Model-free

1. Introduction

In recent years, there has been a growing interest in amorphous semiconductors, especially those known as chalcogenide glasses. This is due to the fact that some amorphous materials show certain unusual switching properties that could be important in modern technological applications such as switching, electrophotography, and memory devices.

Structural studies of chalcogenide glasses are important in determining their transport mechanisms, thermal stability and practical applications. Different techniques have been used to study the structure of chalcogenide glasses, such as scanning electron microscopy (SEM), X-ray diffraction (XRD) and differential scanning calorimetry (DSC) [1–3]. On the other hand, the use of isoconversion methods (model-free) is a trustworthy way of obtaining reliable and consistent kinetic information from both nonisothermal and isothermal data. It can also help to reveal the complexity of multiple reactions due to the dependencies of activation energy on the extent of conversion.

Our recent works with chalcogenide glasses resulted in using isoconversion methods as a reliable way for the calculation of activation energies [1,2,4]. This paper is intended to study the crystallization kinetics of a system containing two peaks. The activation energies of crystallization of $Te_{51.3}As_{45.7}Cu_3$ chalcogenide glass associated to the two peaks were calculated by means of nonisothermal techniques. The effect of annealing on the structure was investigated by SEM.

The system Te–As–Cu attracted considerable attention in the past because of the fact that addition of d-elements, such as Cu, to the chalcogenide glasses causes significant changes in their properties. This may reflect positively on their technological applications.

2. Experimental

2.1. Sample preparation

Bulk material was prepared by the well-established melt-quench technique. High purity (99.999%) Te, As and Cu in appropriate atomic percentage proportions were weighed and sealed in a quartz glass ampoule under a vacuum of 10^{-4} Torr. The contents were heated to about 1250 K for 36 h. During the

* Corresponding author. Tel.: +966 4822 6462; fax: +966 4823 3727.
E-mail address: aaljoraid@taibahu.edu.sa (A.A. Joraid).
[1] On leave from Physics Department, Assiut University, Assiut, Egypt.

0040-6031/$ – see front matter © 2008 Elsevier B.V. All rights reserved.
doi:10.1016/j.tca.2008.02.010

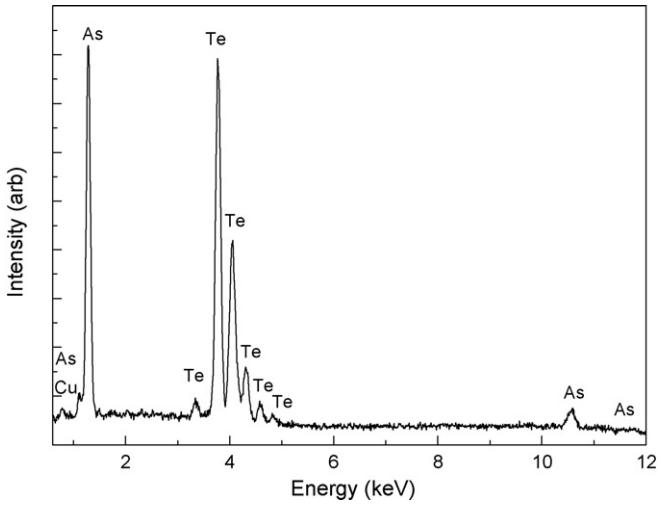

Fig. 1. EDX results of the chalcogenide $Te_{51.3}As_{45.7}Cu_3$.

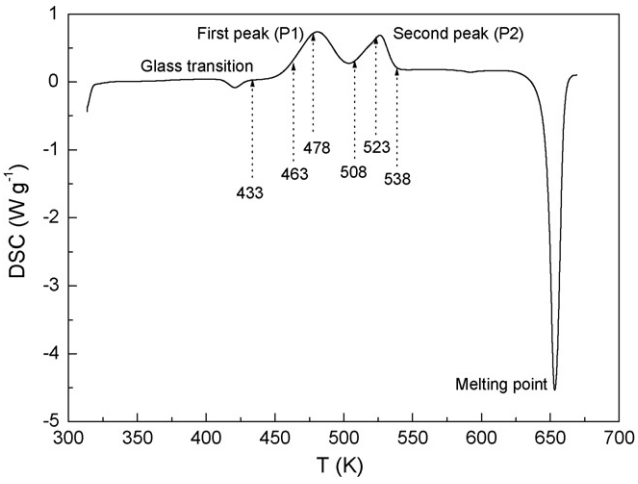

Fig. 2. Typical DSC trace of the chalcogenide $Te_{51.3}As_{45.7}Cu_3$ heated at a constant rate of 30 K min^{-1}. The selected stages of annealing temperature for SEM are shown.

melt process, the tube was frequently shaken to homogenize the resulting alloy.

2.2. Instrumentation

DSC experiments were performed using Shimadzu DSC-60 instrument, with a temperature accuracy of ±0.1 K under dry nitrogen supplied at a rate of 35 ml min^{-1}. The samples, 2–3 mg, were encapsulated in standard aluminum pans. Nonisothermal DSC curves were obtained at selected heating rates between 3 and 99 K min^{-1}. The temperature and enthalpy calibrations were checked with indium (T_m = 429.75 K, ΔH_m = 28.55 J g^{-1}) as a standard material supplied by Shimadzu.

The structure of the samples was examined using a Shimadzu XRD-6000 X-ray diffractometer using Cu K_α radiation (λ = 1.5418 Å). The X-ray tube voltage and current were 40 kV and 30 mA, respectively.

The surface microstructure was revealed by SEM (Shimadzu Superscan SSX-550), and the composition of the alloy was checked by EDX.

3. Results and discussion

3.1. Structural study

Qualitative and quantitative calculations were performed using the EDX technique accomplished with SEM from the displayed characteristic X-ray pattern. The results obtained are shown in Fig. 1. The atomic percentage ratios of Te, As and Cu were found to be 51.3%, 45.7% and 3.0%, respectively.

DSC measurements were conducted on a sample of $Te_{51.3}As_{45.7}Cu_3$ by heating from room temperature to about 700 K, at heating rates of 3–99 K min^{-1}. Fig. 2 shows a typical shape of the obtained results.

The transformation from the amorphous to the crystalline state was investigated by X-ray diffraction measurements performed on samples annealed under isothermal condition. The as-prepared sample was amorphous, as shown in Fig. 3a. Annealing at various temperatures, (T_a), (463, 478 and 518 K) for 15 min increases the sharpness of the lines, indicating grain growth. The presence of a (1 1 2) as a main peak at $2\theta = 29.67^\circ$ could be attributed to As_2Te_3 [JCPDS file 75-1470]. There is a gradual phase change as the temperature goes up (Fig. 3b and c), but a remarkable change occurred at annealing temperature of 518 K where the peak at $2\theta = 30.93^\circ$ nearly disappeared as indicated in Fig. 3d. The two binary crystalline phases Cu–Te and Cu–As with broad composition ranges were recognized at high temperature. For examples of these phases the presence of the two peaks at $2\theta = 27.2^\circ$ and 27.55° which could be attributed to $Cu_{13}Te_7$ [JCPDS file 36-1255]. Also the occurrence of the two peaks at $2\theta = 38.66^\circ$ and 45.89° which could be attributed to Cu_4Te_3 and Cu_2Te, respectively [JCPDS files 42-1253 and 45-1279]. An evidence for the binary crystalline phase Cu–As is the presence of the peak at $2\theta = 43.62^\circ$ which could be attributed to Cu_5As_2 [JCPDS file 21-0279] and the peaks at $2\theta = 50.15^\circ$, 52.61° and

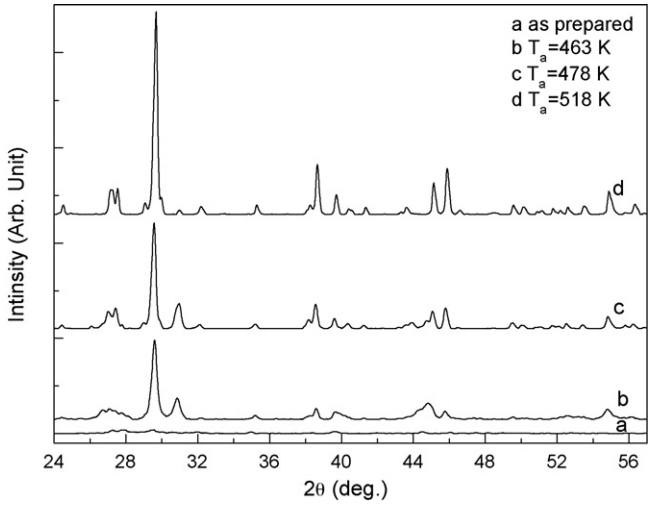

Fig. 3. The XRD patterns of the as-prepared sample and of the annealed samples at different annealing temperatures, T_a.

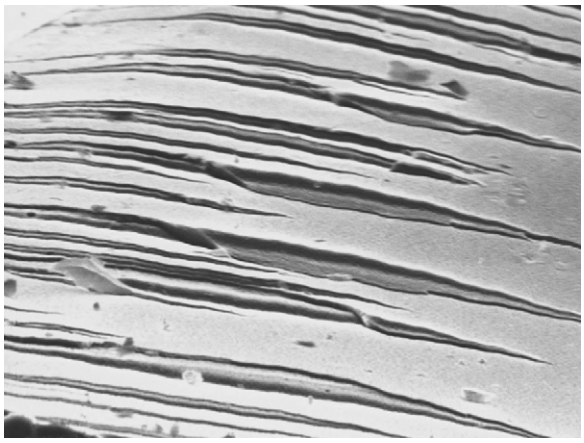

Fig. 4. SEM micrograph of $Te_{51.3}As_{45.7}Cu_3$ as prepared in bulk specimen, ×3000.

53.53° which could be attributed to $Cu_{9.5}As_4$ [JCPDS file 21-0280].

Two exothermic changes were observed: the first one (P1) was between 455 and 500 K for a heating rate of 3–99 K min^{-1}, and the second (P2) from 495 to 542 K for the same heating rate rage. The change in morphology under isothermal annealing was recorded by SEM. The morphology of $Te_{51.3}As_{45.7}Cu_3$ recovered for the as prepared bulk specimen is shown in Fig. 4. The micrograph shows the conchoidal contours, which indicate the glassy state. Fig. 5a–f show the effect of heat treatment on the $Te_{51.3}As_{45.7}Cu_3$ chalcogenide under nitrogen flow. Fig. 5a shows an SEM micrograph of the $Te_{51.3}As_{45.7}Cu_3$ sample after annealing for 15 min at 433 K. The micrograph indicates that the glass structure is still unchanged, but with some distortion. This distortion dramatically increases as temperature increases, accompanied by the beginning of crystallization as shown in Fig. 5b for a sample annealed at 463 K for 15 min. By increasing the annealing temperature to 478 K for 15 min, the crystalline morphology covered the specimen surface and extended into the bulk material as shown in Fig. 5c. The micrograph shows that the crystals have a three-dimensional stack arrangement. As evidenced from Fig. 5d, another phase of crystallization started to developed for the sample annealed at 508 K for the same annealing time. Increasing the annealing temperature to 523 K was accompanied by growth of the crystalline phase, in the form of fine elongated strings as shown in Fig. 5e. These strings form branches and start at centers that are randomly distributed in the medium as shown in Fig. 5f for sample annealed at 538 K for 15 min. The crystalline morphology is homogenous and covers the specimen surface completely.

3.2. Kinetic study

The purpose of this study was to examine the crystallization kinetics and the effect of temperature on the activation energy of $Te_{51.3}As_{45.7}Cu_3$ chalcogenide glass by means of nonisothermal techniques. Model-free isoconversion methods are the most reliable methods for the calculation of the activation energy of thermally activated reactions [4–13]. A large number of isoconversion methods have been conducted for polymer materials, but only a few for studies on chalcogenide glasses.

The assumption that the transformation rate of a solid-state reaction in isothermal conditions is the product of two functions, one dependent on the temperature, T, and the other dependent on the conversion fraction, α, can be generally described by [4–13]:

$$\frac{d\alpha}{dt} = k(T)\ f(\alpha), \tag{1}$$

where $k(T)$ is the reaction rate constant, $f(\alpha)$ is the reaction model, and α is the conversion fraction that represents the volume of the crystallized fraction.

Under nonisothermal conditions with a constant heating rate of $\beta = dT/dt$, the kinetic equation combined with the Arrhenius approach to the temperature function of the reaction rate constant may be rewritten as:

$$\frac{d\alpha}{dT} = \frac{A}{\beta}\exp\left(-\frac{E}{RT}\right)\ f(\alpha), \tag{2}$$

where A (s^{-1}) is the pre-exponential (frequency) factor, E (kJ mol^{-1}) is the activation energy, and R is the universal gas constant.

This equation can be integrated by separation of variables [8,13,14]:

$$\int_0^\alpha \frac{d\alpha}{f(\alpha)} = \frac{A}{\beta}\int_{T_0}^{T}\exp\left(-\frac{E}{RT}\right)dT \approx \frac{AE}{\beta R}\int_0^T \frac{\exp(-y)}{y^2}dy, \tag{3}$$

where T_0 is the initial temperature, $y = E/RT$ and T is the temperature at an equivalent (fixed) state of transformation. The integral on the right-hand side is usually called the temperature integral, $P(y)$, and does not have analytical solution.

$$P(y) = \int_{y_f}^{\infty}\frac{\exp(-y)}{y^2}dy. \tag{4}$$

To solve the temperature integral, several approximations were introduced. In general, all of these approximations lead to a direct isoconversion method in the form of:

$$\ln\left(\frac{\beta}{T^k}\right) = C - \frac{E}{RT}. \tag{5}$$

For each degree of the conversion fraction, α, a corresponding $T_{\alpha i}$ and heating rate are used to plot $\ln(\beta_i / T_{\alpha i}^k)$ against $1/T_{\alpha i}$. The activation energy, E_α, is then determined from the regression slope.

However, the most popular models used for calculation of activation energy are:

1- The Kissinger–Akahira–Sunose (KAS) method [15–17], which takes the form:

$$\ln\left(\frac{\beta_i}{T_{\alpha i}^2}\right) = C_K(\alpha) - \frac{E_\alpha}{RT_{\alpha i}}. \tag{6}$$

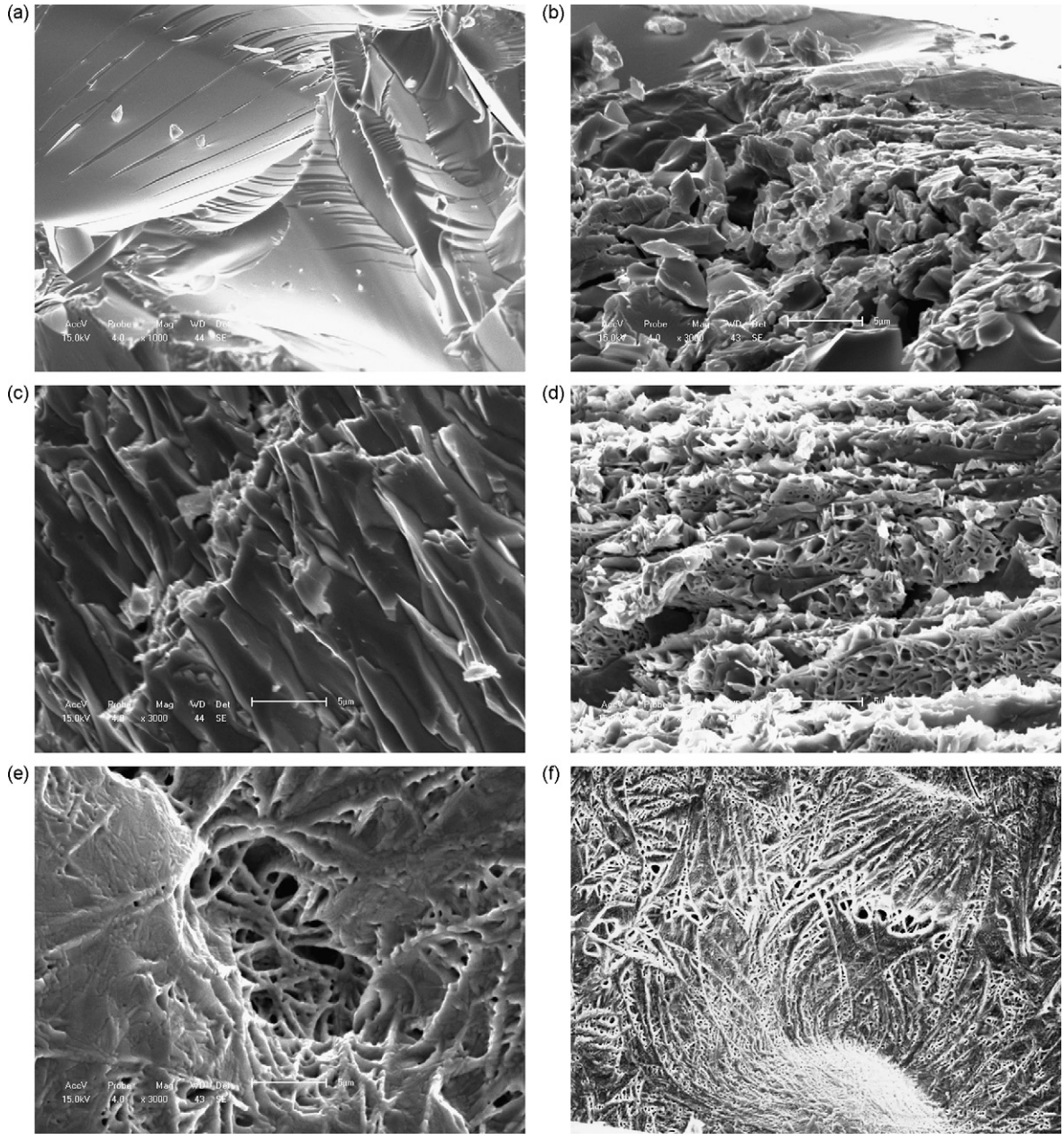

Fig. 5. SEM micrograph of $Te_{51.3}As_{45.7}Cu_3$ annealed for 15 min at different temperatures. (a) Annealed at 433 K, ×1000; (b) annealed at 463 K, ×3000; (c) annealed at 478 K, ×3000; (d) annealed at 508 K; ×3000; (e) annealed at 523 K, ×3000; (f) annealed at 538 K, ×1000.

2- The Flynn–Wall–Ozawa (FWO) method, suggested independently by Flynn and Wall [18] and Ozawa [19]. This method is given by:

$$\ln \beta_i = C_W(\alpha) - 1.0518\frac{E_\alpha}{RT_{\alpha i}}. \quad (7)$$

3- The Tang method. A more precise formula for the temperature integral has been suggested by Tang et al. [20], which can be put in the form:

$$\ln\left(\frac{\beta_i}{T_{\alpha i}^{1.894661}}\right) = C_T(\alpha) - 1.00145033\frac{E_\alpha}{RT_{\alpha i}}. \quad (8)$$

4- The Starink method [8,13], another new method, which is given by:

$$\ln\left(\frac{\beta_i}{T_{\alpha i}^{1.92}}\right) = C_S(\alpha) - 1.0008\frac{E_\alpha}{RT_{\alpha i}}. \quad (9)$$

A second way of extracting the same information is by using the advanced isoconversional method developed by Vyazovkin [21,22]. This method is a nonisothermal method that utilizes an accurate approximation of temperature integral, $P(y)$, which

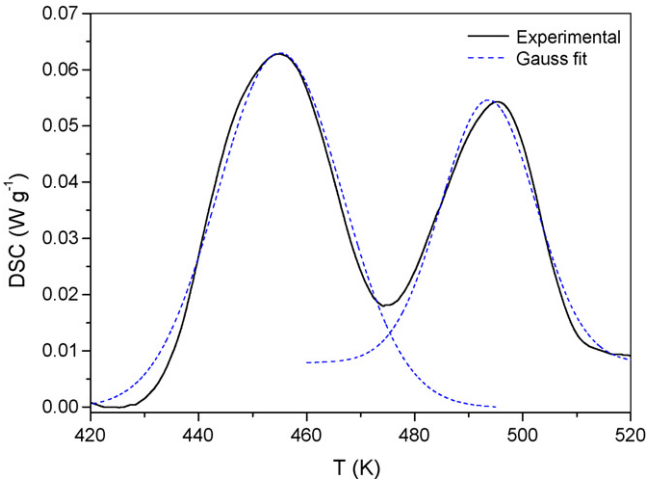

Fig. 6. The separation process for the first (P1) and second (P2) peaks by Gaussian fit, at a constant heating rate of 3 K min^{-1}.

leads to:

$$\Omega = \sum_{i=1}^{n}\sum_{j\neq i}^{n} \frac{I(E_\alpha, T_{\alpha i})\beta_j}{I(E_\alpha, T_{\alpha j})\beta_i}, \tag{10}$$

where n is the number of experiments carried out at different heating rates. The activation energy can be determined at any particular value of α by finding the value of E_α which minimizes the objective function Ω.

The temperature integral, I, was evaluated using an approximation suggested by Gorbachev [23]:

$$\int_0^T \exp\left(\frac{-E}{RT}\right) \mathrm{d}T = \frac{RT^2}{E+2RT} \exp\left(\frac{-E}{RT}\right), \tag{11}$$

The aim of this article is the application of the isoconversional methods mentioned in Eqs. (6)–(10) to evaluate the activation energy for crystallization, $E_\alpha(T)$, and to obtain the dependence of $E_\alpha(T)$ on α and T for all heating rates applied for the glass alloy $Te_{51.3}As_{45.7}Cu_3$.

The most widely used model in obtaining the activation energy for these glasses is the Johnson–Mehl–Avrami (JMA) model for nonisothermal kinetics [24]. This model implies that the Avrami exponent, n, and the activation energy, E, should be constant during the transformation process. Recent papers in this field have shown that n and E are not necessarily constants, but show variation in different stages of the transformation [1,2,4,24].

The first step used in the calculation of the activation energy for crystallization is the separation of the processes for the first (P1) and second (P2) peaks by Gaussian fit as shown in Fig. 6. After this, each peak was treated individually.

Hence, to obtain E, the Kissinger equations (Eq. (6)) was used on a conversion fraction of $\alpha = 0.5$ at different heating rates, β_i. The plots of $\ln(\beta_i/T_{\alpha i}^2)$ against $10^3/T_{\alpha i}$ are shown in Fig. 7 for P1 and P2. It is evident that the data for P1, can be fitted in two regions leading to two different values of the activation energy for crystallization. This gives a good indication that the crystallization reaction follows more than one mechanism for the first peak. The results obtained for P1 gave 177 ± 4 for $\beta < 25$ K min^{-1} and 115 ± 4 kJ mol^{-1} for $\beta > 25$ K min^{-1}. The data for P2, as shown in Fig. 7, indicate a single reaction process that gave a value of E equal to 151 ± 2.

According to the JMA transformation equation, Ligero et al. [25] found the activation energy of crystallization for the alloy $Te_{45}As_{50}Cu_5$ to be equal to 203.15 and 240.8 kJ mol^{-1} for the first and second peak, respectively. By using the Kissinger's equation, Vazquez et al. [26] obtained a value of 222.85 kJ mol^{-1} for E for the composition $Te_{45}As_{45}Cu_{10}$. Via isothermal study of the glass compound $Te_{45}As_{20}Cu_{35}$, Wahab et al. [27] obtained a value of 50.7 kJ mol^{-1} for the first peak. While the second peak gave two distinct values of activation energy for crystallization, for crystallized fraction $\alpha < 0.17$, they obtained a value for E of 218.6 kJ mol^{-1}, and for $\alpha = 0.17$–0.99, the value of E was 32 kJ mol^{-1}.

To evaluate the activation energy for crystallization, $E_\alpha(T)$, the isoconversional methods mentioned in Eqs. (6)–(10) were used on the overall crystallization data to obtain the dependence of $E_\alpha(T)$ on α for all heating rates. By replacing α with the respective temperature interval, the dependencies of E_α on temperature can be obtained [1].

Fig. 8 shows the dependence of E_α on α, for P1 and P2 transformations. The results were obtained by applying the five isoconversional methods (KAS, FWO, Tang, Starink and Vyazovkin) mentioned in Eqs. (6)–(10). The curves show that all methods leads to similar values of E_α.

For P1 the results show that E_α first increases with the extent of conversion, α, then decreases rapidly, approximately linearly in the conversion range of $0.1 \leq \alpha \leq 0.75$. At $\alpha > 0.75$, E_α increases. Three regions were noticed for P2. First an increase of E_α with α followed by a nearly constant value of E_α in the range of $0.3 \leq \alpha \leq 0.6$, and finally, E_α decreases with α. The occurrence of the dependence of E_α on the volume of the crystallized fraction instantly suggests that the data under study follow a multi-step kinetics reaction.

Fig. 9 displays the resulting $E_\alpha(T)$ dependence, as obtained from Eqs. (6)–(10). The values of E_α for P1 are positive and decrease with temperature for all methods used, which simply

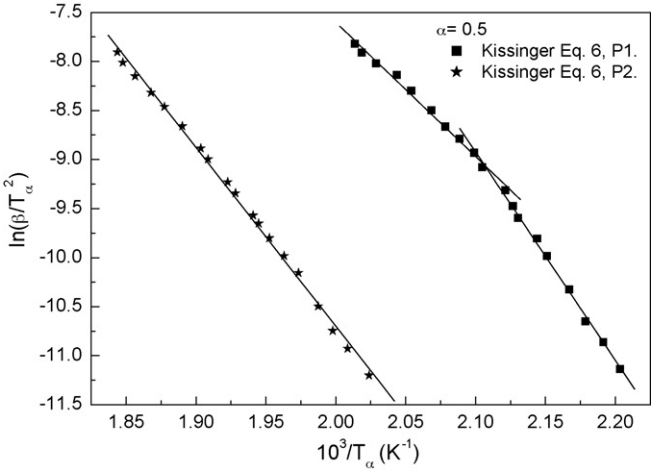

Fig. 7. Experimental plot of first peak (P1) and second peak (P2) of $\ln(\beta_i/T_{\alpha,i}^2)$ vs. $10^3/T_{\alpha,i}$ and a straight regression lines for $\beta = 3$–99 K min^{-1} and $\alpha = 0.5$.

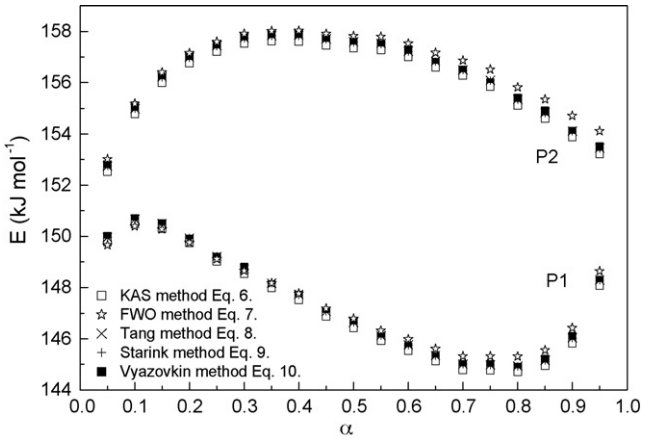

Fig. 8. Dependence of the activation energy for crystallization, E_α, on the volume of the crystallized fraction, α, for P1 and P2.

indicates that the crystallization rate increases with increasing temperature. This behaviour demonstrates that the rate constant of crystallization is, in fact, determined by the rates of two processes: nucleation and diffusion. Because these two mechanisms are likely to have different activation energies, the effective activation energy of the transformation will vary with temperature [28]. This interpretation is based on the nucleation theory proposed by Fisher and Turnbull [29]. According to this theory, the temperature dependence of the crystallization rate, r, is given by:

$$r = r_0 \exp\left(\frac{-E_D}{k_B T}\right) \exp\left(\frac{-\Delta F}{k_B T}\right), \quad (12)$$

where r_0 is the pre-exponential factor, k_B is the Boltzmann constant, E_D is the activation energy for diffusion, and ΔF is the maximum free energy necessary for nucleus formation.

This is also can be confirmed from the results of P1 shown in Fig. 7, which clearly prove that the data in this graph can be fitted to Eq. (6) in two regions, leading to two different values of the effective activation energy. However, the application of Eqs. (6)–(10) on the P2 data indicates that P2 follows a different kinetics reaction model, as shown in Figs. 8 and 9. The fact

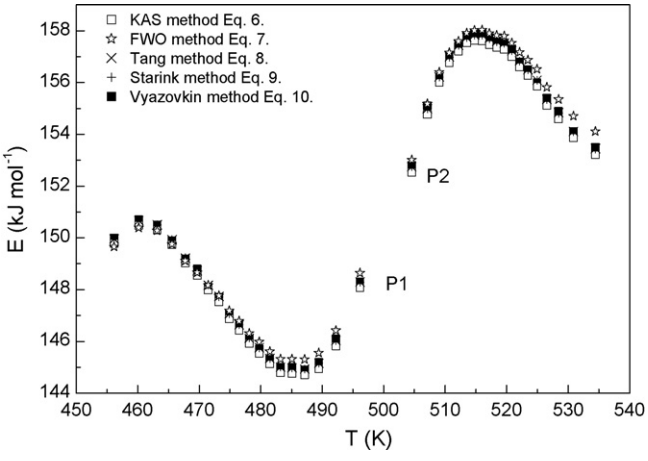

Fig. 9. Dependence of the activation energy for crystallization, E_α, on the temperature for P1 and P2.

Table 1
Common solid-state reaction models used to describe the crystallization process

Model notation	$g(\alpha)$	Mechanism
A1.5	$[-\ln(1-\alpha)]^{2/3}$	Avrami–Erofeev, $n = 1.5$
A2	$[-\ln(1-\alpha)]^{1/2}$	Avrami–Erofeev, $n = 2$
A3	$[-\ln(1-\alpha)]^{1/3}$	Avrami–Erofeev, $n = 3$
A4	$[-\ln(1-\alpha)]^{1/4}$	Avrami–Erofeev, $n = 4$
D1	α^2	One-dimensional diffusion
D2	$(1-\alpha)\ln(1-\alpha)+\alpha$	Two-dimensional diffusion
D3	$[1-(1-\alpha)^{1/3}]^2$	Three-dimensional diffusion (Jander)
F1	$-\ln(1-\alpha)$	First-order reaction
F2	$(1-\alpha)^{-1}-1$	Second-order reaction
P2	$\alpha^{1/2}$	Power law, $n = 1/2$
P3	$\alpha^{1/3}$	Power law, $n = 1/3$
P4	$\alpha^{1/4}$	Power law, $n = 1/4$
R1	α	One-dimensional phase boundary reaction
R2	$1-(1-\alpha)^{1/2}$	Two-dimensional phase boundary reaction
R3	$1-(1-\alpha)^{1/3}$	Three-dimensional phase boundary reaction

that E_α is approximately constant ($0.3 < \alpha < 0.6$) suggests that the examined phase follows single-step kinetics. On other hand, Fig. 7 gives evidence for this assumption, since the fitted results for P2 gave only one value of activation energy for complete heating rate range applied.

This could be a case where, during heating, a sequence of reactions occurs, starting with the formation of a phase (nucleation) at low temperature that is stable below a certain temperature, T_{C1}. This is followed by the formation of another stable phase (P1). As the temperature goes up, another stable phase (P2) develops at T_{C2}. Because the nucleation phase is unstable, we only see the condition as:

Amorphous phase → first phase P1 (stable)

→ second phase P2 (stable)

Therefore, to describe the crystallization process more precisely, and to distinguish which one of the several kinetic models (listed in Table 1) can be used for the process, it will be useful to analyze the integral form of the reaction model, $g(\alpha)$, that is normally used to describe the kinetics of phase transformation in solids [15,30,31]. One can rearrange Eq. (2) and integrate by separation of variables, obtaining the $g(\alpha)$ as:

$$g(\alpha) = \left(\frac{A}{\beta}\right) \int_o^T \exp\left(-\frac{E_\alpha}{RT}\right) \mathrm{d}T. \quad (13)$$

The temperature integral $\left(\int_0^T \exp(-E/RT)\,\mathrm{d}T\right)$ was determined using the Gorbachev approximation shown in Eq. (11). The pre-exponential factor, A, was evaluated by using the so-called artificial isokinetic relationship (IKR) that occurs on fitting various reaction models to the same set of nonisothermal kinetic data.

$$\ln A_j = a + bE_{a,j}. \quad (14)$$

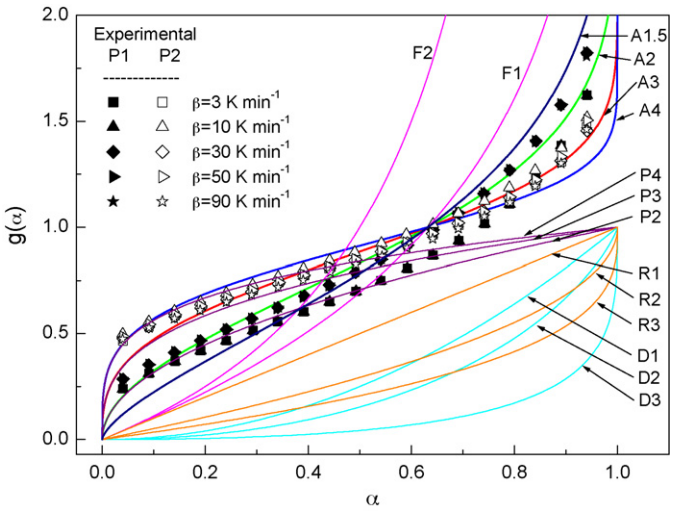

Fig. 10. The variation of $g(\alpha)$ vs. α from model-free analysis (the solid line was calculated from the various theoretical models listed in Table 1).

The subscript, j, refers to one of the possible reaction models $f(\alpha)$ assumed to described the process. Once the parameters a and b have been evaluated, the E_α values are substituted for $E_{a,j}$ in Eq. (14) to estimate the corresponding $\ln A_\alpha$ values. Originally, this procedure was proposed by Vyazovkin for estimating the pre-exponential factor in the isoconversional method [32,33]. Knowing the value of the pr-exponential factor, A_α and the activation energy, E_α, one can reconstruct the reaction model, $g(\alpha)$ numerically form Eq. (13).

The numerically reconstructed experimental kinetic function, $g(\alpha)$, calculated by using Eq. (13), is shown in Fig. 10 for both peaks P1 and P2. The solid line was calculated according to the models listed in Table 1. Comparison of the experimental results with those for the theoretical models can provide information on how and when the reaction mechanism changes during the course of transformation. Without a doubt, it is very clear from Fig. 10 that the reactions follow an Avrami–Erofeev mechanism in the (3–99 K min^{-1}) heating rate ranges. On the other hand, the analysis clearly indicates a change in mechanism for P1 with a change in the heating rate, and this change was found to take place at about $\beta > 25$ K min^{-1}. This is very clear at the later stages of crystallization ($\alpha > 0.4$). At a high heating rate ($\beta > 25$ K min^{-1}) the model-free analysis closely follows A2, with a divergence toward A1.5 at later stage of crystallization ($\alpha > 0.8$). On the other hand, at low heating rate ($\beta > 25$ K min^{-1}) the experimental results only follow A2 at the early stage of crystallization ($\alpha < 0.3$), and they come close to A3 at the later stage ($\alpha > 0.8$). This may give an indication that as the heating rate increases, the crystallization mechanism changes to a lower exponent n. This behaviour may be ascribed to the relative contribution from nucleation and crystal growth. However, as the crystallization process continues toward P2, nucleation may become less and may eventually stop, so that only crystal growth is observed. This may clarify the results of $g(\alpha)$ obtained for P2, where there is no change in mechanism with a change in the heating rate, and the model-free analysis almost follows A3, with a divergence toward A4 at the early stage of crystallization ($\alpha < 0.4$), as shown in Fig. 10. This justification is supported by the values of the activation energies obtained from Fig. 7. Also, the SEM micrograph shown in Fig. 5c and f gives good proof of mechanism changes at different stages of crystallization.

4. Conclusion

The structure and kinetics of crystallization of $Te_{51.3}As_{45.7}Cu_3$ were investigated. The morphology of specimens annealed at selected stages of heat treatments for 15 min showed different crystalline structures. The activation energies of crystallization, $E_\alpha(T)$, were estimated by applying five isoconversional methods, and were found to be strongly temperature dependent. The results show a decrease followed by an increase in the activation energy for crystallization with increasing temperature for P1, while for P2, it is increases with increasing temperature then followed by a decrease. The integral form of the reaction model, $g(\alpha)$, was found to change with heating rate for P1, while it was constant for P2. This behaviour can be explained in light of nucleation theory.

References

[1] A.A. Joraid, Thermochim. Acta 456 (2007) 1.
[2] A.A. Abu-Sehly, A.A. Elabbar, Physica B 390 (2007) 196.
[3] A. El-Korashy, A. Bakry, M.A. Abdel-Rahim, M. Abd El-Sattar, Physica B 391 (2007) 266.
[4] A.A. Joraid, Physica B 390 (2007) 263.
[5] S. Vyazovkin, Thermochim. Acta 355 (2000) 155.
[6] S. Vyazovkin, N. Sbirrazzuoli, Macromol. Rapid Commun. 23 (2002) 766.
[7] S. Vyazovkin, N. Sbirrazzuoli, J. Therm. Anal. Cal. 72 (2003) 681.
[8] M.J. Starink, Thermochim. Acta 404 (2003) 163.
[9] S. Vyazovkin, N. Sbirrazzuoli, Macromol. Rapid Commun. 25 (2004) 733.
[10] A. Khawam, D.R. Flanagan, Thermochim. Acta 436 (2005) 101.
[11] S. Vyazovkin, J. Therm. Anal. Calorim. 83 (2006) 45.
[12] S. Vyazovkin, N. Sbirrazzuoli, Macromol. Rapid Commun. 27 (2006) 1515.
[13] M.J. Starink, J. Mater. Sci. 42 (2007) 483.
[14] B. Jankovic, B. Adnadevic, J. Jovanovic, Thermochim. Acta 452 (2007) 106.
[15] H.E. Kissinger, J. Res. Nat. Bureau Standards 57 (1956) 217.
[16] H.E. Kissinger, Anal. Chem. 29 (1957) 1702.
[17] T. Akahira, T. Sunose, Res. Report Chiba Inst. Technol. 16 (1971) 22.
[18] J.H. Flynn, L.A. Wall, J. Res. Natl. Bur. Stand. Sect. A 70 (1966) 487.
[19] T. Ozawa, Bull. Chem. Soc. Jpn. 38 (1965) 1881.
[20] W. Tang, Y. Liu, H. Zhang, C. Wang, Thermochim. Acta 408 (2003) 39.
[21] S. Vyazovkin, J. Comput. Chem. 18 (1997) 393.
[22] S. Vyazovkin, J. Comput. Chem. 22 (2001) 178.
[23] V.M. Gorbachev, J. Therm. Anal. 8 (1975) 349.
[24] A.A. Joraid, Thermochim. Acta 436 (2005) 78.
[25] R.A. Ligero, J. Vazquez, P. Villares, R. Jimenez-Garay, J. Mater. Sci. 26 (1991) 211.
[26] J. Vazquez, P.L. Lopez-Alemany, P. Villares, R. Jimenez-Garay, Mater. Lett. 5 (1998) 151.
[27] L.A. Wahab, K. Sedeek, A. Adam, Mater. Chem. Phys. 59 (1999) 232.
[28] S. Vyazovkin, I. Dranca, Macromol. Chem. Phys. 207 (2006) 20.
[29] J.C. Fisher, D. Turnbull, J. Chem. Phys. 17 (1949) 71.
[30] P.L. Lopez-Alemany, J. Vazquez, P. Villares, R. Jimenez-Garay, Mater. Chem. Phys. 65 (2000) 150.
[31] G. Chen, C. Lee, Y. Kuo, Y. Yen, Thermochim. Acta 456 (2007) 89.
[32] S. Vyazovkin, Int. J. Chem. Kinet. 28 (1996) 95.
[33] S. Vyazovkin, A. Lesnikovich, Thermochim. Acta 128 (1988) 297.